Host−Guest Chemistry Using an Oriented Mesoporous Host: Alignment and Isolation of a Semiconducting Polymer in the Nanopores of an Ordered Silica Matrix

Junjun Wu, Adam F. Gross, and Sarah H. Tolbert*

Department of Chemistry and Biochemistry, University of California at Los Angeles, Los Angeles, California 90095-1569

Received: October 14, 1998; In Final Form: January 19, 1999

Oriented polymer/silica composites have been synthesized by incorporating the conjugated semiconducting polymer MEH-PPV into the pores of an aligned, hexagonally ordered mesoporous silica. The ordered silica framework is synthesized by a silica/surfactant coorganization process that proceeds via a silicate/surfactant liquid crystalline intermediate. Magnetic fields are used to orient this liquid crystalline intermediate, followed by chemical cross-linking of the silica framework and removal of the surfactant. Hexagonally ordered (p6mm) aligned silica samples are treated with organic chlorosilanes to optimize interactions between the polymer and the silica surface. Polymers are incorporated from solution; thermal cycling is used to drive the polymers into the pores. The resultant polymer incorporation is monitored by polarized photoluminescence spectroscopy. Polymer chains which are oriented in the aligned nanoporous silica show strong polarization anisotropy in their photoluminescence ($I_{VV}/I_{VH} = 4.4$, $I_{HH}/I_{HV} = 0.68$ for vertically oriented pores). Spectroscopic results are compared to the results of a geometric model for transition dipole orientations and used to conclude that as much as 0.8 of the incorporated polymer is isolated within the nanopores of the silica matrix, while as little as 0.2 is located in the macroporous regions formed between grains of the silica host. Intentional oxidation can be used to degrade the polymer not isolated within the porous silica. After oxidation, essentially all of the photoactive polymer appears to be contained within the oriented silica matrix ($I_{VV}/I_{VH} = 5.7$, $I_{HH}/I_{HV} = 0.71$). The results prove that a semiconducting polymer can be isolated within the pores of an ordered silica host and that this isolation can be used to control the optical properties of the guest molecules (in this case the polarization). Further, the ability to simply characterize the degree of polymer incorporation using optical techniques allows us to learn about the effects of processing variables such as the role of surface chemistry, pore size, and thermal cycling on the final degree of polymer incorporation.

Introduction

The discovery that solution phase inorganic species and organic amphiphiles will spontaneously self-organize to form ordered composites has opened up a new avenue for the production of nanostructured materials.[1] These materials consist of domains of self-organized surfactants surrounded by a rigid inorganic framework. In many materials, the organic component can be removed by calcination or ion exchange to produce ordered nano- or mesoporous materials with a pore size and geometry that can be directly controlled by varying readily accessible experimental parameters such as the organic component of the composite, the pH, or the hydrothermal treatment.[2] This versatile, controllable pore structure makes these materials ideal candidates to serve as hosts in nanostructured host/guest composites. A significant body of recent work has shown that disordered sol−gel glasses[3] can act as host matrixes for optically,[4] electrically,[5] and even biologically active[6] guests. Surfactant templated materials share some properties with these sol−gel glasses but in addition provide ordered pores and a narrow pore size distribution. Recent attempts have thus been made to use surfactant templated porous silicas as hosts for new nanostructured composite materials. Efforts have been made to incorporate catalytic clusters,[7−12] confine graphitic carbon,[13] and synthesize semiconductor filaments[14] and polymers[15−17] within the pores of ordered silica matrixes. Potential applications for such composites range from size selective catalysts and chemical sensors to nanoscale electronics. The pores in these hosts can be made as small as 15 Å[1] and as large as 300 Å,[18] a range which nicely spans the diameters of molecular conductors including conducting and semiconducting polymers and aggregates.

While the possibilities are exciting, research in the area of mesopore host/guest chemistry has been hampered by difficulties in characterizing the final composite structure. The major problem frequently is determining the exact location of the guest molecule. Unlike sol−gel glasses, guests are frequently incorporated after formation of the inorganic matrix, thus it is difficult to determine if guest molecules are located within the nanoscale pores of the composite or in the larger macroscale pores that are formed between the randomly arranged grains of the silica host. Even when guest molecules can be incorporated in the synthesis mixture without disrupting the nanoscale order of these materials,[19,20] the exact location of the guest molecules may be unclear.

In this work, we utilize a magnetic field oriented nanoporous silica as our host and incorporate the semiconducting polymer MEH-PPV[21,22] as our guest molecule. The host consists of aggregated domains of ordered, nanoporous silica with a net alignment of the majority of domains along a common orientation direction. This long-range alignment of the pores serves two fundamental purposes. First, it allows us to control the optical, and thus, presumably, the electrical properties of the

10.1021/jp984070s CCC: $18.00
Published on Web 03/16/1999

polymers by polarizing them along the direction of the oriented pores. While this work explores only the optical properties of these host/guest composites, the fact that they are oriented is an important step toward the eventual goal of making electrical contact to isolated polymer chains. The explosion of recent work utilizing these polymers as the active elements of LEDs[23] and even plastic lasers[24,25] emphasizes the importance of these materials for optoelectronic applications. The second, and perhaps practically more important result of using an oriented silica host is that it allows us to quantify the incorporation of guest molecules by determining if the guest displays the same anisotropy as the host. This permits us to explore the molecular interactions, both kinetic and thermodynamic, which allow for incorporation of a polymer guest into a nanoporous silica host.

While this work provides insight into molecular interactions that can be used for the future design of nanostructured materials, it also provides us with a unique opportunity to explore the photophysics of isolated, oriented semiconducting polymers. The complex photophysics of semiconducting polymer films is currently a hotly debated topic, with much of the debate centering around the nature of energy transfer and charge delocalization between polymer chains. By isolating individual chains in an oriented silica matrix, it becomes possible to look at energy transfer only along the polymer backbone without complications from interchain interactions. For example, photoluminescence from dilute MEH-PPV in stretched ultrahigh molecular weight polyethylene indicates enhanced order and electronic delocalization in MEH-PPV,[26] although in this case the role of interchain interactions is less clear due to the potential for phase segregation in polymer blends. It has been proposed that isolating polymer chains can suppress interchain exciton formation, thus enhancing the generation of emissive intrachain species and potentially improving the performance of polymer based optoelectronic devices.[27] A number of recent attempts have also been made to improve device performance by orienting oligomers or polymer chains by various methods. Approaches include stretching−drawing,[28,29] Langmuir−Blodgett technique,[30,31] and vacuum deposition onto friction-transferred poly(tetrafluoroethylene) (PTFE) thin films.[32] Work is currently underway in our laboratory to use transient absorption and emission spectroscopies to learn more about the photophysical properties of the isolated, oriented polymer guests.[33]

In the experiments presented here, the oriented hosts are produced by recently developed techniques,[34] which involve magnetic field alignment[35] of a silicate−surfactant liquid crystalline intermediate[36] followed by chemically induced condensation of the silica framework.[34] After removal of the surfactant template by calcination, alky and arly silyl chlorides are used to treat the pores to optimize favorable interactions between the polymer chains and the host. The silane treatment is critical to the ability to incorporate polymer chains into the nanopores. The polymer we have chosen for these experiments is a substituted poly(phenylenevinylene) (PPV) derivative[37] which is soluble in a range of organic solvents in its fully conjugated form and shows intense photoluminescence.[21,22] Polymers are incorporated from solution, using a combination of chemical and thermal treatments. The resulting composites are not optically clear and thus were index matched in a suitable solvent for optical measurements. Composites are characterized using a combination of two-dimensional X-ray diffraction, ^{2}H NMR spectroscopy, nitrogen adsorption/desorption, scanning electron microscopy, FTIR absorption, optical absorption, and photoluminescence (PL). In particular, polymer orientation is determined using polarized photoluminescence spectroscopy. The results indicate that polymer guests can be incorporated into nanoporous silica hosts and the optical properties of the polymer guest can be polarized by confining them in an oriented host.

Sample Preparation and Experimental Techniques

The synthesis of the aligned silica host has been described in ref 34. It is formed via a lyotropic liquid crystal (LC) intermediate which is prepared by mixing a basic solution of silicate oligomer anions in tetramethylammonium hydroxide (pH $\approx$ 13) with an aqueous cetyltrimethylammonium bromide surfactant solution. This silicate−surfactant LC formed in this way undergoes a phase transition to an isotropic phase at around 80 °C. In our work, $CH_3(CH_2)_{15}N(CD_3)_3Br$ was synthesized from $CH_3(CH_2)_{14}CH_2Br$ and $N(CD_3)_3$ by established methods[2,38] and a small amount of this surfactant was added into the composite so that phase and alignment could be determined by ^{2}H NMR. NMR data were collected on a 7.05 T solid-state MSL 300 spectrometer using a standard quadrupolar-echo pulse sequence with $\pi/2$ pulses of 8.5 μs, a 6 μs echo delay, a 6.7 μs deadtime, a recycle delay of 0.5 s, and 500−8000 signal acquisitions. As the temperature was gradually increased, the initial ^{2}H powder pattern was replaced by a single peak, indicating an isotropic liquid-like state. The sample was cooled slightly and left in the NMR instrument at the temperature of the reversible isotropic-to-anisotropic transition point overnight (usually between 45 and 60 °C). The alignment process was confirmed in situ from the shape of the resulting ^{2}H spectra. Figure 1a shows an example of spectra before and after alignment of the silicate−surfactant liquid crystal. After alignment, the sample was polymerized in HCl vapor for 40 h. Calcination was carried out at 500 °C under flowing N_2, followed by flowing O_2. The final host samples were about a centimeter across and a few millimeters thick in the aligned direction.

The interior surfaces of mesoporous silicas are hydrophilic and freely accessible; approximately 26−30% of the Si atoms carry OH groups.[39] Silylation of the silica was accomplished by treating the calcined mesoporous host with neat chlorosilanes, e.g., phenyldimethlychlorosilane (PDMCS) and trimethylchlorosilane (TMCS). The silica sample was first dried in a vacuum at 100 °C overnight to get rid of residual moisture. It was then placed in a dried test tube capped with a septum and kept under flowing N_2. Triethlyammine was added to catalyze the reaction between silica surface silanol groups and the silane. Pure silane was then injected into the test tube to immerse the sample completely. After about 1 h, the remaining silane liquid was removed and dried heptane was used to wash the silica sample multiple times. The sample was dried in flowing N_2 and then heat treated at 110 °C for phenyldimethylchlorosilane (100 °C for trimethylchlorosilane) for 1 h under N_2 to cure the binding between the silane and the silica wall. Samples were then washed, first with heptane and then ethanol for 1 h each, and dried in a vacuum. The weight increase due to the silylation process was around 50% for PDMCS and 30% when TMCS was used.

To incorporate MEH-PPV into the mesopores, silane-treated silica samples were placed in a ~1% (by weight) polymer in chlorobenzene solution and put in the oven for 48 h at 80 °C. Elevated temperature was used to increase the mobility of the polymer chains, under the assumption that a process like reptation is needed for the polymer chains to snake into the pores of the silica sample.[40] Significantly better incorporation could be achieved when elevated temperatures were used in

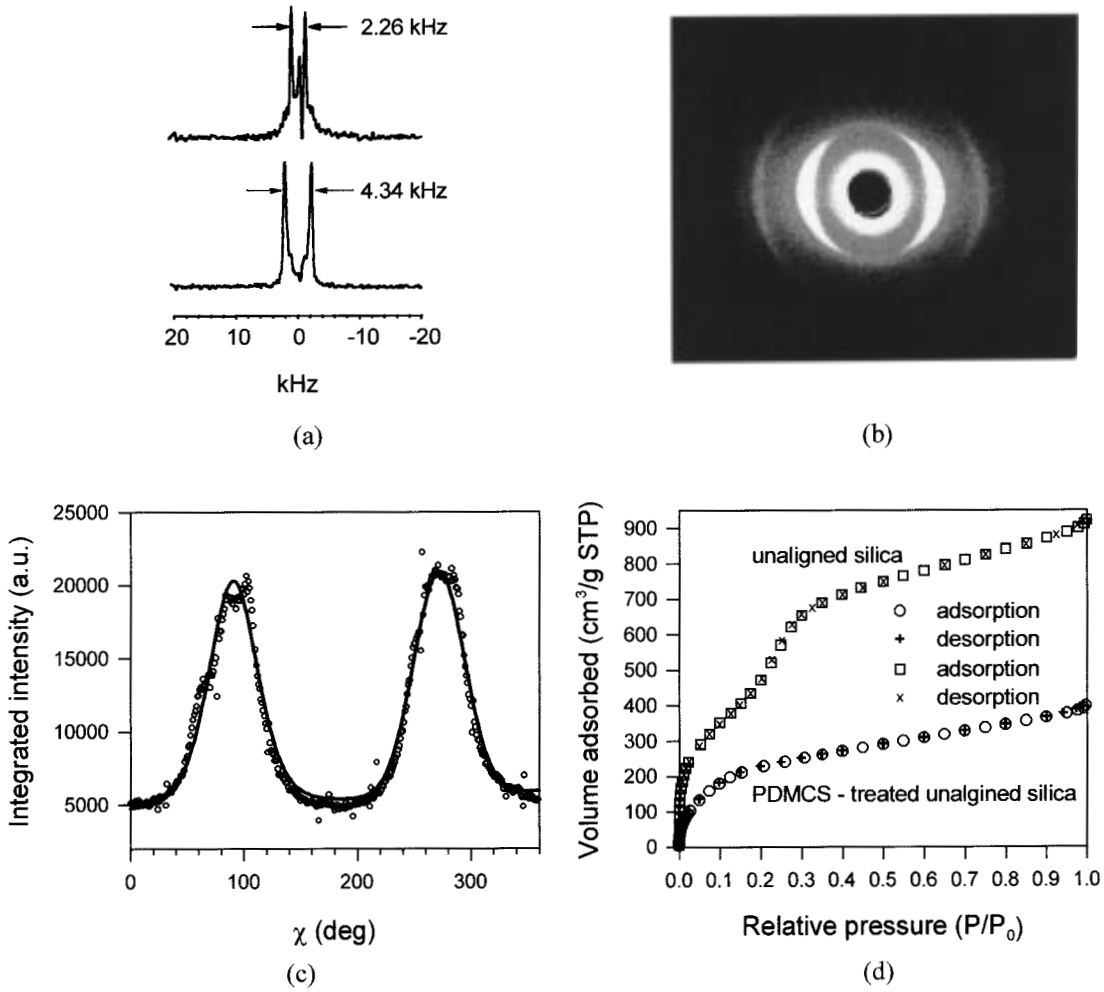

Figure 1. Characterization of aligned mesoporous silica by ^{2}H NMR, 2D XRD, and N2 adsorption/desorption techniques: (a) ^{2}H NMR of sample before (top trace) and after alignment (bottom trace); (b) 2D XRD pattern of the MEH-PPV loaded, PDMCS-treated aligned silica used for fluorescence measurements; (c) angular distribution of pore orientation obtained from (b); (d) N_2 adsorption/desorption of unaligned sample before and after PDMCS treatment.

the synthesis process. The loaded sample was then washed in stirring chloroform for 2 h to remove loosely attached polymer on the exterior surface of the silica and polymer trapped in the large voids between silica grains (this washing time is optimized, as discussed later in the results section). Finally, samples were dried in a vacuum. The net result was a red- or orange-colored solid which was not transparent and thus not ideally suited for optical studies. An index matching solution such as glycerol was used to improve optical quality. Composites were heated in the matching solution at 80 °C until they appeared translucent, a process which usually took a few hours. It was found from 2D XRD that the sample kept its alignment and order after the above treatment. MEH-PPV polymers with molecular weights of approximately 40 000 were used for these experiments, although the chain length distribution was fairly broad.

Dilute MEH-PPV chlorobenzene solutions (~0.01 wt %) were prepared as a comparison to be used in the UV−vis and photoluminescence anisotropy experiments. Neat polymer films were prepared by dissolving MEH-PPV in chlorobenzene at about ~1 wt %. A drop of this solution was then placed on a clean glass slide and the chlorobenzene was evaporated in air.

The instruments used in this work are briefly described in the following section. 2D XRD was used to characterize the periodicity and alignment of the as-synthesized and treated silica. The Cu Kα line of a Rigaku rotating anode X-ray source was used in combination with a Rigaku Raxis II image plate detector. Typical scan times were 16 min. The porosity of the materials was measured using a Micrometrics ASAP 2000 porosimeter. Isotherm plots of unaligned silica were measured both before and after silane treatment. UV−vis absorption was measured using a Spectral Instruments, Inc. spectrophotometer. FTIR measurements utilized a Perkin-Elmer Paragon 1000 FT-IR spectrometer, and SEM images were obtained on a Cambridge Instruments Stereo Scan S25 microscope using samples which were sputter coated with approximately 600 Å of gold. Photoluminescence anisotropy experiments utilized the 488 nm line of an Ar^+ laser for excitation in combination with a Princeton Instruments intensified diode array detector. The sample in the index matching solution was held in a glass cuvett with the pores oriented in the vertical direction. Optical polarization (both excitation and detection) was determined and controlled using a combination of linear polarizing films, a rotating quartz linear polarizer, and birefringent $\lambda/4$ and $\lambda/2$ sheet retarders. Linearly polarized photoluminescence was converted into circularly polarized light before focusing into the monochromator to prevent transmission bias from the vertically ruled gratings. In later sections of this paper, I_V (I_H) will be used to represent the total photoluminescence (PL) intensity observed with excitation polarized parallel (perpendicular) to the pores. I_{VH} specifies the PL intensity with vertical excitation polarization and horizontal detection polarization. I_{VV}, I_{HH}, and I_{HV} are defined in a similar manner.

Results and Discussions

a. Silica Framework. The alignment of the silicate−surfactant liquid crystal is indicated by the ^{2}H NMR powder pattern.[34,35] Domains oriented parallel to the applied field show a splitting of 4.34 kHz, approximately twice that of the dominant 2.26 kHz splitting observed in the unaligned powder pattern, which shows a distribution of orientations with a cusp corresponding to domains oriented perpendicular to the applied field (Figure 1a). The alignment of the resultant nanoporous silica is further determined from the 2D XRD image (Figure 1b). Porous silica samples with a hexagonal structure show strong anisotropy with significantly increased scattering intensity for domains (pores) aligned parallel to the magnetic field direction. The azimuthal dependence of scattering intensity of the (100) peak is obtained to quantify alignment of the pores (Figure 1c). We find an angular distribution of the pore orientation between 35° and 50°, fwhm. The exact width depends on the details of the temperature cycling during alignment (50° in Figure 1c). We also find that neither silane treatment nor polymer loading significantly affects the hexagonal periodicity or pore alignment of the composites as determined by 2D XRD, although the (100) diffraction peak does broaden after treatment. Figure 1b shows a typical 2D X-ray diffraction pattern of a sample after silane treatment and polymer incorporation. Three hexagonal peaks can be seen as well as clear anisotropy in the diffraction pattern. The sample is sitting with pores oriented approximately vertically in the laboratory frame.

Nitrogen adsorption analysis of unaligned MCM-41 mesoporous silica before silane treatment shows single-point surface areas at a relative pressure (P/P_0) of 0.20 as high as 1600 m^2/g and total pore volumes up to 1.4 cm^3/g at a relative pressure of 0.99 (Figure 1d). The typical deflection (knee) of mesoporous materials is clear at a partial pressure of about 0.3 P/P_0. The lack of hysteresis in the isotherm is also consistent with a uniform (and fairly small) pore material. After treatment with phenyldimethlchlorosilane (PDMCS), the surface area drops to 780 cm^2/g and the volume to 0.61 cm^3/g. In the isotherms of the silane-treated samples, the knee observed in bare mesophase silica is not visible, presumably because the pore size has moved into the micropore regime. At relative pressures above 0.3, however, both isotherms follow the same trend, slightly rising with no significant steps or jumps. We thus believe that the pore size of silica after silane treatment goes into the micropore region and that the sample still preserves much of its original porosity.[41] FTIR data (not shown) of vacuum-dried, phenyldimethylsilane-treated samples in a KBr pellet indicate characteristic phenyl stretches (701, 731, 831 cm^{-1}). In addition, the Si−OH vibration at 964 cm^{-1} completely disappears after silane treatment, further confirming the binding of our arylsilanes to the porous silica surface.[42] From the results of 2D XRD, nitrogen adsorption, and IR spectroscopy, we conclude that magnetic field oriented mesoporous silicas can be silane treated and then incorporated with polymer without loss of the long-range hexagonal periodicity or uniaxial orientation of the mesopores. The next task we undertake is to prove that the incorporated polymer is actually situated within the nanopore environment and thus shows anisotropic behavior.

b. Polymer Incorporation. The UV−vis spectra of free and incorporated MEH-PPV are shown in Figure 2. Dilute solutions of MEH-PPV show two absorption bands, one centered around 500 nm and the other near 330 nm. A typical UV−vis spectrum of the polymer-loaded, silane-treated, aligned silica is also shown. In this experiment, the pores of the sample are oriented parallel to the propagation of the incoming beam because of restrictions in the dimensions of the sample, which is only about 2 mm thick along the aligned direction. The silica matrix has an absorption peak around 300 nm. After subtraction of the silica background, it can be seen that absorption from MEH-PPV in the silane-treated silica matrix is very similar to that observed in solution with no significant shifts in absorption maxima. Only minor broadening and intensity changes are seen in the absorption bands of the host/guest composite as compared to the solution phase spectra. Broadening and intensity changes of this type are typical of an inhomogeneous environment and are similar to those seen in MEH-PPV films. These results allow us to conclude that fundamental optical properties of the polymer are preserved upon incorporation.

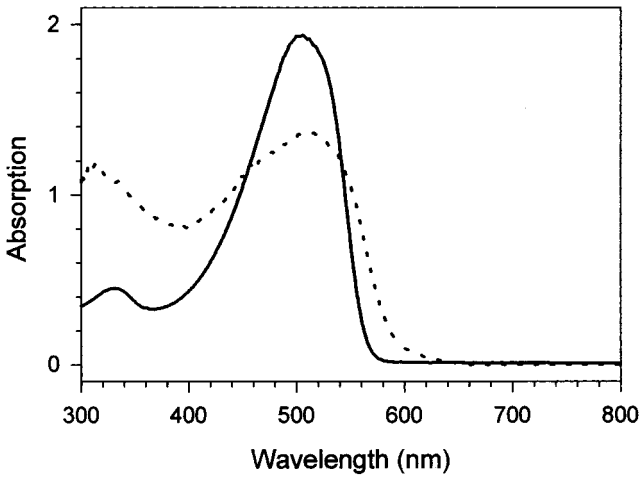

Figure 2. UV−vis absorption spectra of dilute MEH-PPV in a chlorobenzene solution (solid line) and the same MEH-PPV sample incorporated into PDMCS-treated aligned silica, index matched in glycerol (dashed line). A background due to the pure silica host has been subtracted from the composite absorption spectra. The concentration of the solution is about 0.2 mg/mL.

Polymer orientation is probed primarily using polarized photoluminescence spectroscopy. This technique can be used to determine the distribution of absorbing and emitting dipoles in a sample. If dipole orientation can be simply related to molecular orientation, this technique provides a straightforward spectroscopic way to ascertain the physical distribution of molecular orientations. For example, we have collected polarized fluorescence from dilute 4-dicyanomethylene-2-methyl-6-*p*-dimethylaminostyryl-4H-pyran (DCM)/polystyrene (0.05wt %) films. When vertically polarized incident light is used, the intensity ratio between vertically (I_{VV}) and horizontally (I_{VH}) polarized photoluminescence is 2.9, a value close to theoretical value of 3.0 for a random distribution and discrete fluorescent molecules ($\langle\cos^2\theta\rangle = 1/3$). Essentially the same value is obtained when comparing I_{HH} to I_{HV}.

Parts a and b of Figure 3 show photoluminescence spectra obtained from a 0.05% (wt) solution of MEH-PPV in chlorobenzene. The angular dependence of PL polarization is shown in part c, normalized with respect to the highest value. Dilution of the polymer solution does not change the PL spectra or the ratios observed in polarized PL experiments, indicating that polymer chains are isolated. From Figure 3, it can be seen that the photoluminescence is isotropic and polarized in the direction of the incident beam, $I_{VV}/I_{VH} \cong I_{HH}/I_{HV} \cong 1.7$. This value differs significantly from the value of ∼3 observed and predicted for DCM/polystyrene films. The explanation for this probably lies in the dynamics of energy transfer in dilute semiconducting polymer solutions. In such dilute solutions where polymer chains are well separated, excitations will be localized to single chains

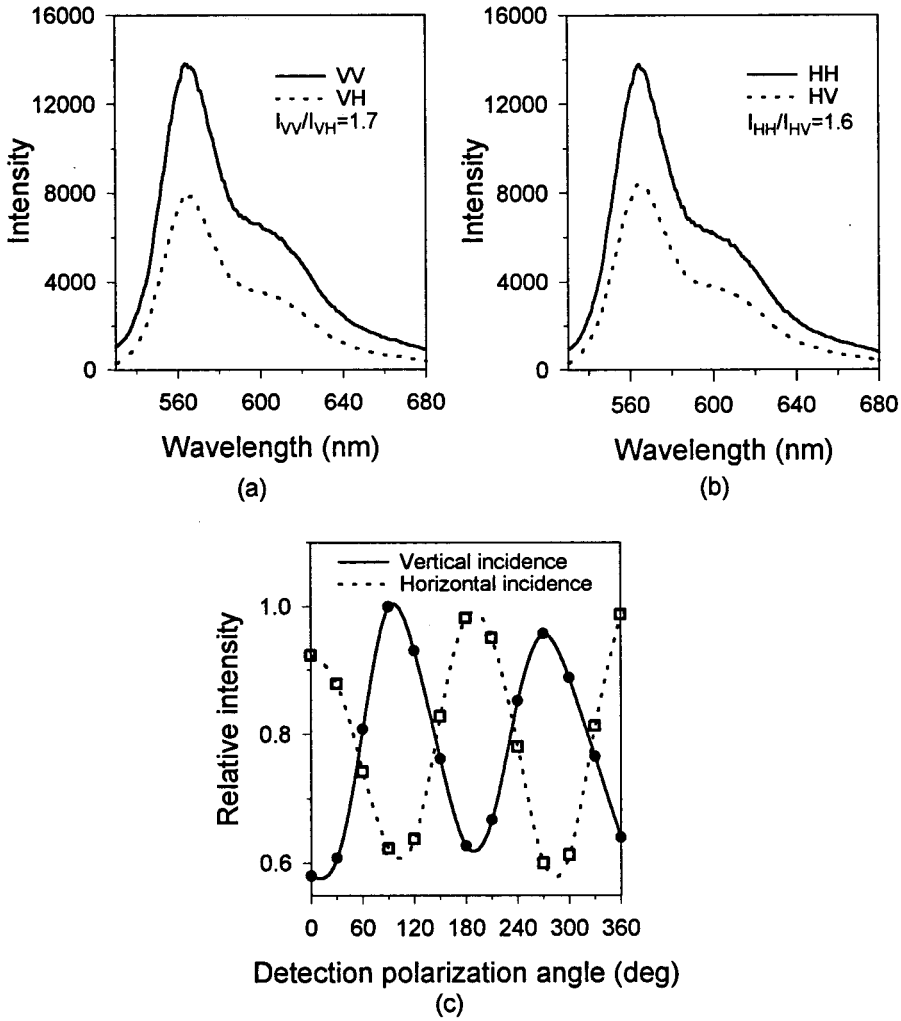

Figure 3. Fluorescence from 0.05% MEH-PPV in chlorobenzene solution: (a), (b) fluorescence spectra; (c) angular dependence of PL intensity.

TABLE 1: Fluorescence Polarization Anisotropy Ratios of Different Samples

	MEH-PPV in chlorobenzene solution	MEH-PPV film	MEH-PPV in PDMCS-unaligned silica	MEH-PPV in PDMCS-aligned silica	MEH-PPV in TMCS-aligned silica	MEH-PPV in bare aligned silica	oxidized MEH-PPV in treated, aligned silica
I_{VV}/I_{VH}	1.7	1.4	1.8	3.8−4.0	4.2−4.4	1.7	5.3−5.7

but should be able to migrate along the chain or hop between different segments of the same chain. When chains are coiled, as they appear to be in solution,[43] this migration results in a loss of polarization. Some polarization may also be lost due to polymer tumbling, although this effect should not be large, given the size of these polymers and their fast radiative lifetimes.[44]

In contrast to dilute solutions, the polarization ratio (e.g., I_{VV}/I_{VH}) of neat MEH-PPV films is only about 1.4. In these films, which show moderate conductivity,[45] polymer chains overlap and excitations can transfer between chains with different orientations, resulting in increased polarization loss.[27] When polymers are incorporated into *randomly oriented*, phenylsilane (PDMCS)-treated silica hosts, the polarization ratio is around 1.8. The value is notably higher than that observed in neat polymer films (1.4), where energy transfer between polymer chains should be a significant mechanism for polarization loss. The value of 1.8 is still lower than the theoretical value of 3.0, probably due to combination of residual polymer located outside the silica nanopores and some excitation migration as in solution. In addition, for reasons that we do not yet fully understand, unaligned composites cannot be index matched as well as oriented ones, and thus some polarization is lost simply due to multiple scattering of the excitation and fluorescent light. These numbers serve as benchmarks for understanding the photoluminescence anisotropy for our oriented, nanostructured polymer/silica composites. Fluorescence polarization anisotropy ratios for MEH-PPV in different environments are summarized in Table 1.

When phenylsilane (PDMCS)-treated *aligned* silica is used as the matrix for the MEH-PPV, there is clear anisotropy in the emitted photoluminescence as shown in Figure 4. In this experiment, the long axes of the silica pores are oriented vertically in the laboratory frame and thus vertically polarized incident light should be approximately parallel to the transition dipoles of polymers oriented within those pores. From parts a and b of Figure 4 it can be seen that luminescence is preferentially emitted along the direction of the pore orientation, suggesting that at least part of the polymer molecules are indeed aligned inside the pores. This is emphasized in Figure 4b by the fact that luminescence is preferentially emitted with vertical polarization, despite the fact that the sample is excited with horizontally polarized light. Polarization ratios as high as 4.4 (I_{VV}/I_{VH}) and as low as 0.68 (I_{HH}/I_{HV}) have been observed in these oriented samples. Figure 4c more clearly states this trend

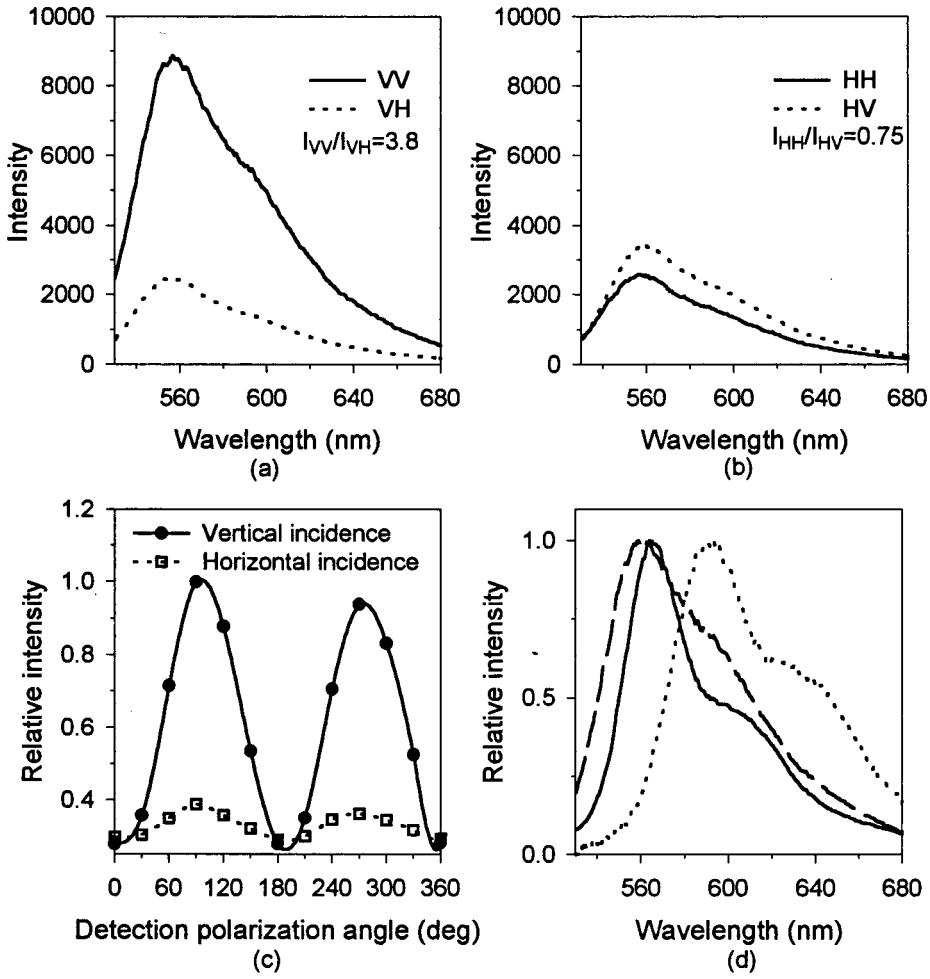

Figure 4. Fluorescence from MEH-PPV in phenyldimethlchlorosilane-treated aligned nanoporous silica: (a), (b) fluorescence spectra; (c) angular dependence of PL intensity. In (d), the VV PL of a polymer solution, a pristine film, and polymer in aligned silica are compared with intensity normalized to maximum values: solid line, 0.01% MEH-PPV in chlorobenzene solution; dotted line, pristine MEH-PPV film on glass slide; dashed line, MEH-PPV in PDMCS-treated aligned silica matrix.

by plotting the angular dependence of the polarization angle for both vertically and horizontally excited composites. In sharp contrast to the isotropic behavior shown in Figure 3c, there is a dramatic difference depending on whether the excitation polarization is parallel or perpendicular to the pore orientation direction. As seen in parts a and b of Figure 4, total fluorescence is significantly higher when the excitation polarization is parallel to the pore axis. It should be noted that this effect is not due to different penetration depth (and thus absorption) of the vertical and horizontal excitation light, an effect that has been observed in stretched film systems. In our case, the sample is optically thick for both horizontally and vertically polarized light.[46]

Despite the clear anisotropy, there is still significant horizontally polarized luminescence from our vertically oriented samples, which needs to be explained. There are a number of explanations for the observed depolarization, all of which are likely important in our samples. First of all, as shown by the 2D XRD (Figure 1, parts b and c), there is an angular distribution (~50°) in the orientation of the pores of the silica matrix, with some fraction of the pores being randomly oriented (~27%). Many excitations must therefore be created on chains located in pores which are not perfectly parallel to the excitation polarization. These excitations have a significant probability of emitting light polarized perpendicular to the excitation polarization. Added to the physical distribution of polymer/pore orientations, recent experiments indicate that the transition dipoles in these polymers are actually oriented about 20° off the chain axis.[28,46] This off-axis angle will effectively broaden the physical distribution already present in our composite samples (see appendix for details). The second source of horizontally polarized fluorescence is a small amount of polymer in our composites that is not contained within the silica nanopores, but rather in the larger macropores between silica grains. These polymer molecules would be in an environment similar to a neat polymer film and thus should display very little anisotropy, regardless of incident polarization direction.

A final polymer configuration that could affect polarization ratios in a complicated way that cannot be excluded is the possibility that chains are partly situated in the oriented pores and partly dangling in the voids between silica grains. In this case, depending on the dynamics of energy transfer along the polymer chains, excitations created outside the pores could possibly migrate onto the straighter polymer segments inside the pore, thus increasing vertically polarized luminescence. A detailed analysis of the excitation transfer mechanism from transient absorption and emission experiments will be discussed in a future paper.[33]

In an effort to determine if there were large amounts of polymer contained in the macropores of these samples (second option discussed above), we employed scanning electron microscopy (SEM). From the SEM images, we confirmed the existence of micrometer-sized voids between the silica single

grains (domains). No polymer aggregates, however, could be observed in the voids on the micrometer scale in the aligned, silane-treated polymer/silica composites. This, of course, does not exclude the situation discussed above where the polymer molecules reside in the pores with part of the chain sticking out. A final possibility that must be ruled out is that the silica grain structure somehow reflects the overall pore orientation and thus simply sticking to the outsides of such aligned grains could align the polymer. SEM images, however, show that the micron-sized grains of aligned hexagonal phase silica are not elongated in any preferential direction (image not shown here). Even though some of the polymer may form aggregates in the voids between these grain they are not aligned and thus will only lower the observed depolarization ratio according to the fraction of polymer contained in the macropores compared to the chains incorporated inside aligned nanopores. From these results, we conclude that the anisotropy observed in the polarized luminescence is due to the alignment of polymer chains situated inside of oriented silica nanopores.

From geometric considerations, we can further hypothesize that there must be only one polymer chain per silica nanopore. By combining X-ray diffraction and nitrogen absorption/desorption, it is possible to show that the diameter of the silica pores is about 22 Å.[34] Recent studies have shown that when trimethylsilyl groups are bound to the insides of silica pores, a decrease in pore diameter of 5−6 Å is observed.[47,48] When phenyldimethylsilyl groups are utilized instead, the diameter decreases by about 7 Å.[47] If one assumes similar coverage of our silyl groups, this leaves a pore diameter of only 15−17 Å, depending on surface treatment, for the polymer chain. Although substituted PPV polymers are notoriously noncrystalline, recent powder diffraction studies on MEH-PPV suggest a *close packed* chain diameter of approximately 8−9 Å. This leaves a fairly tight fit in the available space, and thus it is highly unlikely that any two chains could simultaneously occupy the same pore. This then argues that not only are chains oriented by incorporation into silica nanopores but that they are also completely isolated from each other and separated by an approximately 20 Å thick wall of organosilane and glass. As discussed below, this isolation should play an important role in the photophysics of our incorporated polymer chains.

Preliminary transient absorption experiments can also be used to argue that oriented polymer chains are, in fact, isolated in the pores of our silica host.[33] Transient absorption is a measure of excited-state lifetime and thus can be used as a rough measure of the fluoresce lifetime in these polymers. In dilute solutions, polymers are observed to have long (∼300 ps) lifetimes, presumably because excitations cannot hop between neighboring polymer chains.[27,44] In PPV films, in contrast, transient absorption lifetimes are much shorter and not single exponential.[27] Preliminary data shows that for pores oriented vertically in the laboratory frame, with vertically polarized probe light, long lifetimes almost identical to those seen in solution samples are observed with a high *S*/*N* ratio. For the small amount of signal that can be obtained with horizontally polarized probe light, short excited-state lifetimes are observed, characteristic of aggregated polymer chains. These results confirm our hypothesis that vertically oriented polymer chains are isolated in the pores of the silica host. They further suggest that some nonincorporated polymer is present in the composites.

In Figure 4d, luminescence spectra from dilute polymer solutions, neat polymer films, and our polymer/aligned silica composites are shown. The photoluminescence spectra of the MEH-PPV incorporated in the aligned silica matrix is broader than that observed in solution due to inhomogeneous broadening; similar effects were observed in optical absorption (Figure 2). Significant broadening, however, is also observed in the pristine polymer films where polymers again occupy an inhomogeneous environment. The red shift in the film luminescence is likely dominated by self-absorption of luminescence from the blue edge of the film and by energy transfer between polymer chains. Excitation transfer is an energy-driven process which results in a reduction in luminescence energy with each hop. The fact that luminescence from the composite (I_{VV}) is quite similar to that observed in solution is further confirmation that the majority of polymer chains in the composite are isolated and thus excitation transfer between chains is not observed.

c. Chemistry of Polymer Incorporation. Efforts were made to determine what steps in the synthesis process were the most important for polymer incorporation and what type of molecular interactions dominated the process. It was found that silylation is indispensable in changing the properties of silica walls (polarity, hydrophobicity) and adjusting the interaction between the polymer molecules and wall surface. Without silane treatment the surface of the silica is hydrophilic. While there may be some favorable interactions between the polymer alkoxy side chains and the framework surface silanol groups, these polymers are generally hydrophobic and thus are not expected to interact favorably with the silica framework. The polymers are expected to minimize these unfavorable interfacial interactions by adopting a coiled configuration. This is clearly exemplified in the following experiment: MEH-PPV is incorporated into bare aligned silica following the same procedures used for silane-treated aligned samples. The PL spectra are shown in Figure 5. The polarization ratio in the vertical direction, $I_{VV}/I_{VH} = 1.7$, is much lower than that observed in the silane-treated aligned sample and similar to the unaligned sample, suggesting little orientation of the polymer chains. As a more sensitive measure of alignment, the polarization ratio in the horizontal direction, $I_{HH}/I_{HV} = 1.4$, is almost the same as in the vertical direction, in sharp contrast to the silane-treated samples which consistently show a value less than 1.0 for I_{HH}/I_{HV}. In addition to the loss of anisotropy in PL, the spectra are red-shifted approximately 30 nm compared to the silane-treated aligned sample, resulting in a peak frequency very close to that observed in neat polymer films. From these results, we conclude that only a small portion the polymer chains, or a small fraction of many polymer chains, are aligned inside the silica pores with the remaining polymers coiled (and probably interacting) on the surface of the silica host. After silane treatment, however, the silica surface becomes hydrophobic, producing a more ideal interaction between the polymers and the framework. Similar results have been observed in the intercalation of hydrophobic polymers into the gallery regions of silica clays. Here as well, organic modifiers are required for efficient polymer incorporation.[49]

The interfacial interaction between the host matrix and guest molecules can be tuned by varying properties of the silanes such as the size and the polarizability. While MEH-PPV is soluble in benzene, it is insoluble in alkanes. It could thus be expected that a difference should exist between the degree of alignment achievable with the phenyldimethylchlorosilane (PDMCS) and with trimethylchlorosilane (TMCS)-treated samples. When TMCS is used to treat the aligned silica, however, a higher anisotropy in emitted fluorescent is obtained ($I_{VV}/I_{VH} = 4.4$, $I_{HH}/I_{HV} = 0.68$ for TMCS treatment compared to $I_{VV}/I_{VH} = 4.0$, $I_{HH}/I_{HV} = 0.75$ for PDMCS treatment). The solubility under space confined condition could be quite different from that observed in bulk solution. Alternatively, the need for hydro-

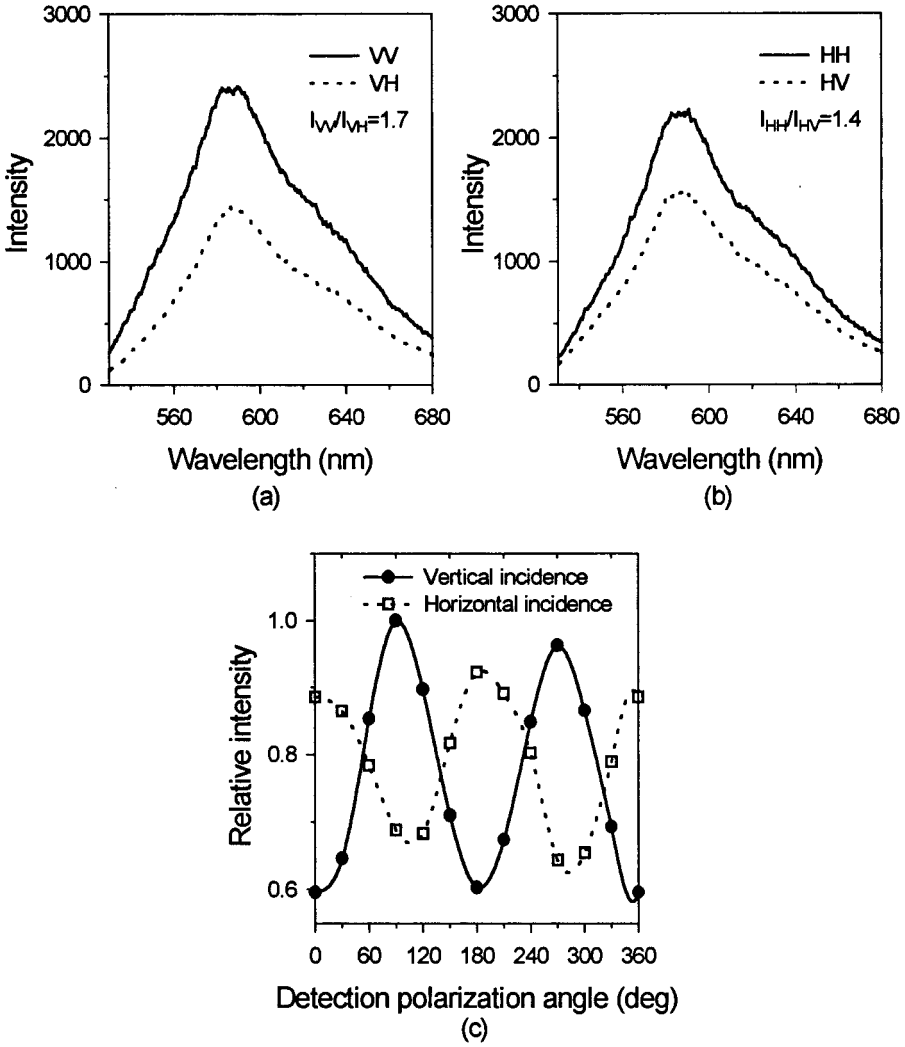

Figure 5. Fluorescence from MEH-PPV in bare aligned nanoporous silica: (a), (b) fluorescence spectra; (c) angular dependence of PL intensity.

phobic interactions could be adequately satisfied by both silanes, but by simple geometric packing arguments, the smaller trimethyl groups may favor facile incorporation of polymer over the bulky phenyldimethyl substituents. In addition to size effects, overly favorable interactions between the PDMCS and the conjugated polymer could also slow the kinetics of incorporation by effectively increasing the friction between the polymer and the pore wall. Such effects have been observed in the intercalation of polymers into silica clays.[50] As with many complex processes, a balance is needed between thermodynamic driving force for reaction and the kinetic barriers which restrict that process. The criteria for good host/guest (mesoporous matrix and conjugated polymer in this case) interactions can thus perhaps be summarized as a combination of polarity differences and space-filling effects. The polarity of host and guest should be matched while avoiding strong interactions between host and guest. The size of the pores should be optimized for facile incorporation of guest polymer molecules.

Washing away free polymer is a key feature of this incorporation mechanism. As seen in Figure 6, the degree of anisotropy steadily increases with washing time up to about 2 h, after which it appears to stabilize. As observed in our experiment, the polarization ratio starts to fall after washing times of approximately 8 h. It is envisioned that, at early times, unincorporated polymer chains are more easily solvated by the washing solution and so are preferentially washed away, leaving behind the incorporated chains. This produces a net increase in polarization anisotropy. With time, however, polymer chains can actually be drawn out of pores and into solution, stopping the increase in anisotropy and even reversing the trend. Some differences have been observed between samples washed in chlorobeneze and those washed in chloroform, suggesting that the details of this process can affect the final degree of polarization anisotropy.

The washing results suggest that polymer not located in the confines of the nanopores causes a reductions in polarization anisotropy. We have thus made efforts to reduce luminescence from unincorporated polymer to see how this affects the overall anisotropy of the sample. The intentional oxidation of the silica/polymer composites by exposure to air is a simple chemical method which can be employed to do this. Oxidized PPV and its derivatives are know to show reduced luminescence efficiencies due to a large increase in fluorescence quenching sites.[51,52] If one assumes that polymers located within the silica pores are less accessible to oxygen than polymers on external surface of silica due to space confinement, this process should enhance luminescence from the oriented component of the composite relative to the unoriented material. Experiments involving intentional oxidation do appear to produce an increase in polarization anisotropy. For example, experiments were carried out on both PDMCS- and TMCS-treated samples which initially showed depolarization rations of $I_{VV}/I_{VH} = 4.0$, $I_{HH}/I_{HV} = 0.78$ for PDMCS and $I_{VV}/I_{VH} = 4.4$, $I_{HH}/I_{HV} = 0.68$ for TMCS. After 2 months in contact with air in a glycerol solution, the ratios

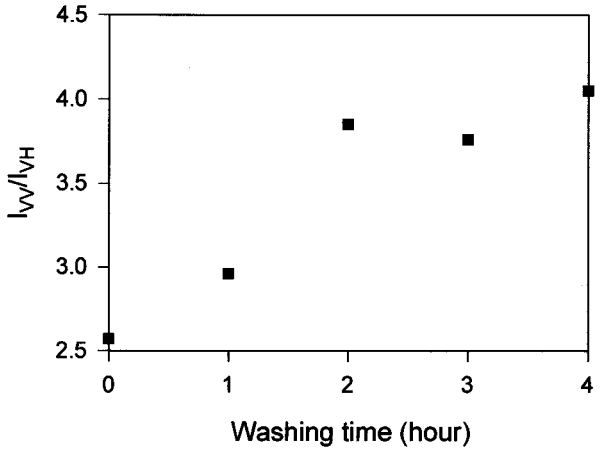

Figure 6. Relation between fluorescence polarization ratio and washing time. Samples were washed in stirring chloroform for different time.

had changed to $I_{VV}/I_{VH} = 5.3$, $I_{HH}/I_{HV} = 0.88$ and $I_{VV}/I_{VH} = 5.7$, $I_{HH}/I_{HV} = 0.71$ for PDMCS- and TMCS-treated samples, respectively. At the same time, the intensity of fluorescence from the sample was virtually constant over 2 months. These results suggest that polymers incorporated within the confines of our silica nanopores were, in fact, protected from oxidation. This result is particularly important as oxidation damage is a major issue with polymer LED devices.[52]

d. Quantifying Polymer Incorporation and Polymer Distributions. Our knowledge of the silica framework pore distribution (Figure 1c) allows us to quantify the fraction of oriented polymer chains in our composites based on the total fluorescence polarization anisotropy. The expected fluorescence anisotropy, that is, I_{VV}/I_{VH} and I_{HH}/I_{HV}, can be calculated from the square of the dot product of the electric field vector and the polymer transition dipole moment for both absorption of the incident light and the subsequent luminescence. This term corresponds simply to the probability of luminescence with a given polarization. Because we are considering only vertically and horizontally polarized incident and luminescent light, these dot products are simply a series of sine and cosine terms. By integrating over the actual pore distribution, which can be obtained from curve fitting of the data presented in Figure 1c, the expected polarization ratios can be calculated. Note that this distribution is not identical in all samples (although it is always similar) and thus variations in the degree of pore alignment introduces some error into our calculations. Matters are made somewhat more complicated by recent results on stretched PPV films.[46] From this work, the authors conclude that the transition dipole in these materials is actually about 20° off the polymer backbone. We have included this 20° term by assuming a random distribution of transition dipoles, all 20° off the polymer axis. The details of the calculations are presented in the Appendix.

This model, however, makes the assumption that the transition dipole is fixed with respect to the molecule and so is the same for both absorption and luminescence. This assumption is not always valid in our systems. For example, the photoluminescence produced upon vertically polarized excitation can arise from four possible sources: (1) straight chains inside aligned pores, (2) straight chains inside unaligned pores, (3) aggregated polymer between silica grains, and (4) excitation transfer into (or out of) pores from polymers that are situated partly inside and partly outside of the pores. Among these possibilities, options 1 and 2 are explicitly considered by our model. Option 3 can be included separately, leaving only excitation transfer from outside the pores to the inside (or vice versa) as a process that cannot be addressed by our model. For the time being, this process will thus be ignored. The fraction of sample outside the pores is likely to consist of domains of agglomerated polymer, and thus a value of 1.4 can be used for I_{VV}/I_{VH} and I_{HH}/I_{HV} for this fraction of the polymer sample (Table 1).

From analysis of the 2D XRD image in Figure 1b, we find that about 73% of the silica host is aligned in the general direction of our applied magnetic field (fwhm = 50°) and 27% of the silica host is a randomly oriented hexagonal phase.[53] Using these numbers, our calculations predict a vertical anisotropy, I_{VV}/I_{VH}, of 5.2 and a horizontal anisotropy, I_{HH}/I_{HV}, of 1.65 (Appendix). As discussed above, our model does not include the effects of energy migration along the polymer chains, which can potentially account for some differences between our calculated values and the experimental numbers. Our experimental anisotropy values are quite high for vertically polarized excitation light, however, and are fairly close to the values predicted from our model. We thus conclude that most of the chains excited with vertically polarized light are straight and isolated within the pores and thus the effect of excitation migration should be minimal for the vertically oriented component of the sample. We therefore use I_{VV}/I_{VH}, as opposed to I_{HH}/I_{HV}, when calculating fractions of incorporated polymers based on our polarization model. To achieve the experimental values of $I_{VV}/I_{VH} = 4.0$ observed for PDMCS-treated samples, we must assume that 0.7 of the polymer in our sample is isolated within the nanopores of our silica host, while 0.3 is located in the macroporous voids between grains. For the more highly polarized TMCS-treated samples, the I_{VV}/I_{VH} value of 4.4 corresponds to 0.8 of the polymer isolated within the nanopores and only 0.2 contained in the macroporous voids between domains. If excitation migration is directional from outside the pores to the inside, the addition of this effect would only enhance observed anisotropy. In that case, our value of 0.8 incorporated polymer would then be considered an upper limit for our samples.

Upon oxidation in air, however, polarization anisotropy increases to $I_{VV}/I_{VH} = 5.3$ for the PDMCS-treated samples and to 5.7 for the TMCS-treated composites. Both of these numbers are in good agreement with the calculated value of $I_{VV}/I_{VH} = 5.2$, indicating that virtually all of the optically active polymer in our oxidized samples is isolated within the porous silica host. The fact that experimental values for the oxidized TMCS-treated sample are in some cases higher than the calculated values could be due to the directional energy transfer discussed above. Alternatively, this sample may have a slightly narrower silica pore orientation distribution than the samples shown in Figure 1 and used in our calculations. A narrow pore orientation distribution would produce a slightly higher limiting luminescence polarization anisotropy. The oxidation results also show that incorporated polymers are protected from oxidation, probably by imposing restrictions on the diffusion of oxygen into the filled pores. This fact could become important for device applications of these composite materials. These results thus show both that polymer chains can be incorporated into a nanoporous silica host in an oriented manner and that we can quantify the degree of incorporation by comparing polarized optical spectroscopy with a simple model for polymer polarization.

Conclusions

In this paper, we have shown that it is possible to incorporate single semiconducting polymer chains into the nanopores of an

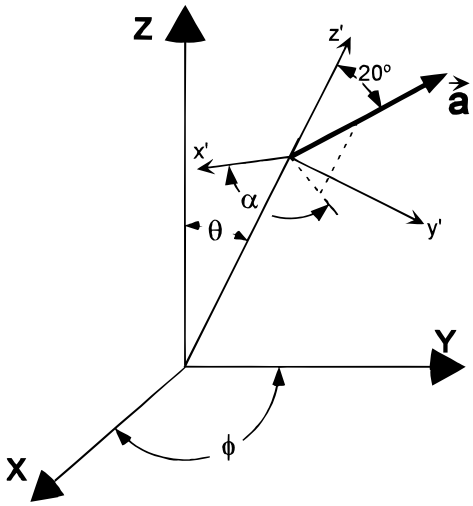

Figure 7. The orientation of polymer unit dipole moment in our model system.

oriented silica host. By incorporating polymer in this way, it is possible both to orient and isolate the polymer chains. Polarized photoluminescence spectroscopy combined with geometric modeling allows us to quantify the degree of polymer orientation; current results indicate that approximately 0.8 of the incorporated polymer chains are isolated within the silica. We can also use these experiments to learn about the factors that are important to polymer incorporation. From our results, it appears that a good polarity match between polymer and host is required. Size considerations, however, also appear to be important as exemplified by the fact that larger polarization ratios can be obtained with trimethylchlorosilane-treated samples than with phenyldimethylchlorosilane treatment. Thermal treatment is required to overcome kinetic barriers and allow polymers to snake down into the pores. Finally, it is likely that incorporation is facilitated by the long range π conjugation in PPV polymers. This conjugation makes the polymer behave locally like a rigid rod and thus reduces the entropic penalty of polymer incorporation.

These results are of fundamental interest for understanding the dynamics of incorporation of polymers into confined geometries. Because we are using a semiconducting polymer, however, the results also have significant practical implications. Single polymer chains, isolated in an insulating matrix but spaced as closely as 2 nm from each other, mark the true molecular limit of a conducting wire array or an array of electroluminescent chromophores, depending on how the polymer is doped. The fact that the array is periodic further means that individual elements could someday be addressed. While the possibility for making devices is admittedly a fair step away, the possibilities for learning about the photophysics of polymers in this geometry are exciting and immediate. In particular, the long-standing question of single chain conductivity in semiconducting polymers can be addressed by such measurements as ultrafast optical absorption and emission or AC microwave conductivity, both of which are currently under investigation. These results show that by combining an oriented host with an understanding of the molecular interactions between host and guest molecules, it is possible to make composite materials with new and potentially interesting optical properties. As both the ability to create oriented nanoporous hosts and the means of incorporating guest molecules increase, this area is likely to dramatically increase the options for the production of nanostructured optoelectronic materials.

Acknowledgment. The authors gratefully acknowledge the help of Prof. F. Wudl and Dr. R. Helgeson for both the synthesis of the MEH-PPV samples used here and much advice on its properties. The authors also thank Prof. B. J. Schwartz for many helpful discussions on the photophysics of PPV-based polymers. Assistance from Dr. M. J. Strouse in NMR spectroscopy is greatly appreciated. Acknowledgment is made to the donors of the Petroleum Research Fund, administered by the American Chemical Society, for support of this research.

Appendix

In our calculation, a transition dipole moment in the polymer chain is represented by an arbitrary unit vector $\vec{a}$ as in Figure 7. This vector makes an angle of 20° with the axis z', which is an arbitrary vector in the distribution of the silica pore orientations. The angle between x' and the projection of $\vec{a}$ into the $x'y'$ plane is α. After transformation from the $x'y'z'$ to the **XYZ** coordinate system, the components of the vector $\vec{a}$ in **XYZ** system are found to be the following:

$$\mathbf{a}_x = \sin\phi \sin\alpha \sin(20) + \cos\phi \cos\theta \cos\alpha \sin(20) + \cos\phi \sin\theta \cos(20) \quad \text{(A.1)}$$

$$\mathbf{a}_y = -\cos\phi \sin\alpha \sin(20) + \sin\phi \cos\theta \cos\alpha \sin(20) + \sin\phi \sin\theta \cos(20) \quad \text{(A.2)}$$

$$\mathbf{a}_z = -\sin\theta \cos\alpha \sin(20) + \cos\theta \cos(20) \quad \text{(A.3)}$$

From Figure 1c in the text of this paper, the pore orientation is fit with a Pearson function of the following form with a linear baseline:

$$G(\theta) = \frac{a_0}{\left[1 + 4\left(\frac{\theta - a_1}{a_2}\right)^2 (2^{1/a_3} - 1)\right]^{a_3}} \quad \text{(A.4)}$$

The parameters are given in Table 2. The linear background is due to a combination of scattering from unaligned nanoporous hexagonal silica and random scattering of the direct beam, mostly from the air. After subtracting the fraction of the background due to random scattering from the direct beam, this distribution (Pearson function plus remaining linear background) is used in the following integration to calculate the polarization ratios by averaging over the distribution of silica pore orientations and all angles of α

$$I_{VV} \propto \int_0^{360}\int_0^{180}\int_0^{360} a_z(\alpha,\theta)^4 G'(\theta) \sin(\theta)\, d\alpha\, d\theta\, d\phi \quad \text{(A.5)}$$

$$I_{VH} \propto \int_0^{360}\int_0^{180}\int_0^{360} \times a_y(\alpha,\theta,\phi)^2 a_z(\alpha,\theta)^2 G'(\theta) \sin(\theta)\, d\alpha\, d\theta\, d\phi \quad \text{(A.6)}$$

In eqs A.5 and A.6, G' is used to represent the distribution function with the random scattering background subtracted. The ratio between I_{HH} and I_{HV} can be calculated in a similar way. For our experimental distribution, $G'(\theta)$, results show $I_{VV}/I_{VH} = 5.2$ and $I_{HH}/I_{HV} = 1.6$. The deviation of the second ratio from the experimental data (~0.8) is intriguing. This is probably due to shortcomings in our static model where excitation transfer

TABLE 2: Fitting Parameter of Pore Orientation in Aligned Silica

	a_0 (height)	a_1 (center)	a_2 (fwhm)	a_3
peak 1	14728	0.00	52.6	100
peak 2	16371	182	50.9	100

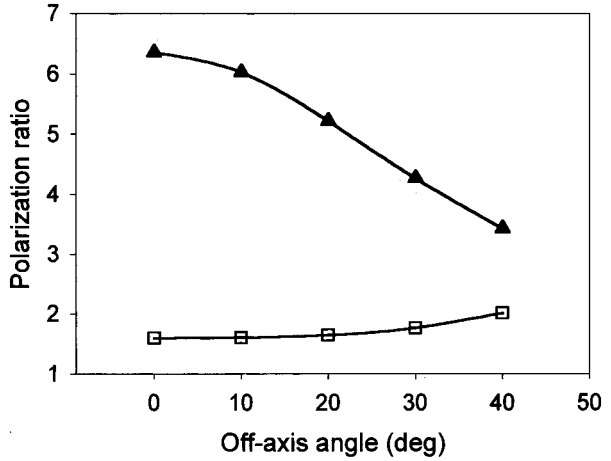

Figure 8. Relationship between polarization ratios and off-axis angle from calculation: (▲) I_{VV}/I_{VH}; (□) I_{HH}/I_{HV}.

from outside the pores into aligned pores (or vice versa) due to excitation transfer along the polymer chains is not considered. For the majority of the polymer chains that are oriented and confined within the pores, however, the requirement of rigid molecules and constant absorption and emission transition dipole moment orientation is more or less satisfied. We thus feel that it is reasonable to use this model to calculate oriented fractions of polymers using the I_{VV}/I_{VH} term.

To see the effect of the off-axis angle on the polarization ratios, we varied this angle between 0° and 30°; the result is shown is Figure 8. The ratio of I_{VV}/I_{VH} is more dependent on the off-axis angle than the ratio of I_{HH}/I_{HV}. An off-axis angle of about 20° was used because it was predicted by independent measurements on stretched MEH-PPV/polystyrene films.[46] The results indicate that for our oxidized samples essentially all of the optically active polymer is isolated within the silica pores. The experimental values for I_{VV}/I_{VH} ranging from 5.3 to 5.7 (after oxidation in air) are in reasonable agreement with the calculated value of 5.2.

References and Notes

(1) Kresge, C. T.; Leonowitz, M. E.; Roth, W. J.; Vartuli, J. C.; Beck, J. S. Na*ture* **1992**, *359*, 710. Beck, J. S.; Vartuli, J. C.; Roth, W. J.; Leonowicz, M. E.; Kresge, C. T.; Schmitt, K. T.; et al. *J. Am. Chem. Soc.* **1992**, *114*, 10834.

(2) Hou, Q.; Margolese, D. I.; Stucky, G. D. *Chem. Mater*. **1996**, *8*, 1147.

(3) Counio, G.; Esnouf, S.; Gacoin, T.; Boilot, J.-P. *J. Phys. Chem*. **1996**, *100*, 20021. Akbarian, F.; Dunn, B. S.; Zink, J. I. *J. Phys. Chem*. **1995**, *99*, 3892. Levy, D.; Esquivias, L. *Adv. Mat*. **1995**, *7*, 120.

(4) Canva, M.; Georges, P.; Perelgritz, J. F.; Brum, A.; Chaput, F.; Boilot, J. P. *Appl. Optics* **1995**, *34*, 428. Schaudel, B.; Guermeur, C.; Sanchez, C. *J. Mater. Chem*. **1997**, *7*, 61.

(5) Wei, Y.; Yeh, J. M.; Jin, D.; Jia, X.; Wang, J. *Chem. Mater*. **1995**, *7*, 969.

(6) Braun, S.; Rappoport, S.; Zusman, R.; Avnir, D.; Ottolenghi, M. *Mater. Lett.* **1990**, *10*, 1.

(7) Maschmeyer, T.; Rey, F.; Sankar, G.; Thomas, J. M. *Nature* **1995**, *378*, 159. Zhou, W. Z.; Thomas, J. M.; Shephard, D. S.; Johnson, B. F. G.; Ozkaya, D.; Maschmeyer, T.; Bell, R. G.; Ge, Q. *Science* **1998**, *280*, 705.

(8) Junges, U.; Schuth, F.; Schmid, G.; Uchida, Y.; Schlögl, R. *Ber. Bunsen-Ges. Phys. Chem.* **1997**, *101*, 1631. Schuth, F. *Ber. Bunsen-Ges. Phys. Chem.* **1995**, *99*, 1306.

(9) Walker, J. V.; Morey, M.; Carlsson, H.; Davidson, A.; Stucky, G. D.; Butler, A. *J. Am. Chem. Soc*. **1997**, *119*, 6921.

(10) Yamamoto, T.; Shido, T.; Inagaki, S.; Fukushima, Y.; Ichikawa, M. *J. Phys. Chem. B* **1998**, *102*, 3866. Yamamoto, T.; Shido, T.; Inagaki, S.; Fukushima, Y.; et al. *J. Am. Chem. Soc.* **1996**, *118*, 5810.

(11) Okumura, M.; Tsubota, S.; Iwamoto, M.; Haruta, M. *Chem. Lett*. **1998**, 315. Eswaramoorthy, M.; Neeraj; Rao, C. N. R. *Chem. Commun.* **1998**, 615.

(12) Aronson, B. J.; Blanford, C. F.; Stein, A. *Chem. Mater*. **1997**, *9*, 2842.

(13) Wu, C.-G.; Bein, T. *Science* **1994**, *266*, 1013.

(14) Leon, R.; Margolese, D. I.; Stucky, G. D.; Petroff, P. M. *Phys. Rev. B* **1995**, *52*, R2285.

(15) Wu, C.-G.; Bein, T. *Science* **1994**, *264*, 1757.

(16) Moller, K.; Bein, T.; Fischer, R. X. *Chem. Mater*. **1998**, 10, 1841. Moller, K.; Bein, T. In *Mesoporous Molecular Sieves 1998, Studies in Surface Science and Catalysis, V. 1117*; Bonnevoit, L., Beland, F., Giasson, S., Kaliaguine, S., Eds.; Elsevier Science: Amsterdam, 1998.

(17) Frisch, H. L.; Mark, J. E. *Chem. Mater*. **1996**, *8*, 1735.

(18) Zhao, D. Y.; Feng, J.; Huo, Q.; Melosh, N.; Fredrickson, G. H.; Chmelka, B. F.; Stucky, G. D. *Science* **1998**, *279*, 548.

(19) Honma, I.; Zhou, H. S. *Chem. Mater*. **1998**, *10*, 103.

(20) Lim, M. H.; Blanford, C. F.; Stein, A. *Chem. Mater*. **1998**, *10*, 467. Lim, M. H.; Blanford, C. F.; Stein, A. *J. Am. Chem. Soc*. **1997**, *119*, 4090.

(21) Poly(2-methoxy-5-(2′-ethylhexyloxy)-1,4-phenylenevinylene): Motamedi, F.; Ihn, K. J.; Ni, Z.; Srdanov, G.; Wudl, F. *Polymer* **1992**, *33*, 1102.

(22) Wudl, F.; Srdanov, G. U.S. Patent 5, 189, 136, 1993.

(23) Burroughes, J. H.; Bradley, D. D. C.; Brown, A. R.; Marks, R. N.; Mackay, K.; Friend, R. H.; Burn, P. L.; Holmes, A. B. *Nature* **1990**, *347*, 539.

(24) Tessler, N.; Denton, G. J.; Friend, R. H. *Nature* **1996**, *382*, 695.

(25) Hide, F.; Diaz-Garcia, M. A.; Schwartz, B. J.; Andersson, M. R.; Pei, Q.; Heeger, A. J. *Science* **1996**, *273*, 1833.

(26) Hagler, T. W.; Pakbaz, K.; Voss, K. G.; Heeger, A. J. *Phys. Rev. B* **1991**, *44*, 8652.

(27) Yan, M.; Rothberg, L. J.; Kwock, E. W.; Miller, T. M. *Phys. Rev. Lett*. **1995**, *75*, 1992.

(28) Hagler, T. W.; Pakbaz, K.; Heeger, A. J. *Phys. Rev. B* **1994**, *49*, 10968.

(29) Weder, C.; Sarwa, C.; Bastiaansen, C.; Smith, P. *Adv. Mater*. **1997**, *9*, 1035.

(30) Sluch, M. I.; Pearson, C.; Petty, M. C.; Halim, M.; Samuel, I. D. W. *Synth. Met.* **1998**, *94*, 285.

(31) Pal, A. J.; Ostergard, T. P.; Osterbacka, R. M.; Paloheimo, J.; et al. *IEEE J. Quantum Electron.* **1998**, *4*, 137.

(32) Gill, R. E.; Hadziioannou, G.; Lang, P.; Garnier, F.; Wittmann, J. C. *Adv. Mater.* **1997**, *9*, 331.

(33) Doan, V.; Wu, J.; Tolbert, S. H.; Schwartz, B. J. Manuscript in preparation.

(34) Tolbert, S. H.; Firouzi, A.; Stucky, G. D.; Chmelka, B. F. *Science* **1997**, *278*, 264.

(35) Firouzi, A.; Schaefer, D. J.; Tolbert, S. H.; Stucky, G. D.; Chmelka, B. F. *J. Am. Chem. Soc*. **1997**, *119*, 9466.

(36) Firouzi, A.; Kumar, D.; Bull, L. M.; Besier, T.; Sieger, P.; Huo, Q.; Walker, S. A.; Zasadzinski, J. A.; Glinka, C.; Nicol, J.; Margolese, D.; Stucky, G. D.; Chmelka, B. F. *Science* **1995**, *267*, 1138.

(37) Heeger, A. J.; Kivelson, S.; Schrieffer, J. R.; Su, W.-P. *Rev. Mod. Phys.* **1988**, *60*, 781.

(38) Menger, F. M.; Littau, C. A. *J. Am. Chem. Soc.* **1993**, *115*, 10083.

(39) Landmesser, H.; Kosslick, H.; Storek, W.; Fricke, R. *Solid State Ionics* **1997**, *101*−*103*, 271.

(40) Doi, M.; Edwards, S. F. *J. Chem. Soc., Faraday Trans. 2* **1978**, *74*, 1789.

(41) See, for example: Gregg, S. J.; Sing, K. S. W. *Adsorption, Surface Area and Porosity*, 2nd ed.; Academic Press: New York, 1982. Ravikovitch, P. I.; Haller, G. L.; Neimark, A. V. In *Mesoporous Molecular Sieves 1998, Studies in Surface Science and Catalysis, V. 1117*; Bonnevoit, L., Beland, F., Giasson, S., Kaliaguine, S., Eds.; Elsevier Science: Amsterdam, 1998.

(42) Boccuzzi, F.; Coluccia, S.; Ghiotti, G.; Morterra, C.; Zecchina, A. *J. Phys. Chem*. **1978**, *82*, 1298.

(43) Gettinger, C. L.; Heeger, A. J.; Drake, J. M.; Pine, D. J. *J. Chem. Phys.* **1994**, *101*, 1673.

(44) Solution radiate lifetimes for MEH-PPV are around 300 ps; see ref 27.

(45) Lee, C. H.; Yu, G.; Moses, D.; Heeger, A. J. *Phys. Rev. B* **1994**, *49*, 2396. Barth, S.; Bässler, H.; Rost, H.; Hörhold, H. H. *Phys. Rev. B* **1997**, *56*, 3844.

(46) Hayes, G. R.; Samuel, I. D. W.; Phillips, R. T. *Phys. Rev. B* **1997**, *56*, 3838.

(47) Andwander, R.; Palm, C.; Stelzer, J.; Groeger, O.; Engelhardt, G. In *Mesoporous Molecular Sieves 1998, Studies in Surface Science and Catalysis, V. 1117*; Bonnevoit, L., Beland, F., Giasson, S., Kaliaguine, S., Eds.; Elsevier Science: Amsterdam, 1998.

(48) Zhao, X. S.; Lu, G. Q. *J. Phys. Chem. B* **1998**, *102*, 1556.

(49) Vaia, R. A.; Ishii, H.; Giannelis, E. P. *Chem. Mater*. **1993**, *5*, 1694.

(50) Vaia, R. A.; Giannelis, E. P. *Macromolecules* **1997**, *30*, 8000.

(51) Rothberg, L. J.; Yan, M.; Papdimitrakopoulos, F.; Galvin, M. E.; Kwock, E. W.; Miller, T. M. *Synth. Met.* **1996**, *80*, 41.

(52) Yan, M.; Rothberg, L. J.; Papadimitrakopoulos, F.; Galvin, M. E.; Miller, T. M. *Phys. Rev. Lett.* **1994**, *73*, 744.

(53) This is in agreement with previous results; see ref 34.